ACS OMEGA

http://pubs.acs.org/journal/acsodf

Article

Structural and Functional Characterization of Novel Phosphotyrosine Phosphatase Protein from *Drosophila melanogaster* (Pupal Retina)

Rubina Naz, Asma Saeed, Vineet Tirth, Neeraj Kumar Shukla, Abdulilah Mohammad Mayet, Alamzeb Khan, Narcisa Vrinceanu,* Mihaela Racheriu, Tahira Amir, and Anwar Iqbal*

Cite This: *ACS Omega* 2023, 8, 1937−1945

Read Online

ACCESS | Metrics & More | Article Recommendations | Supporting Information

ABSTRACT: A novel pair of protein tyrosine phosphatases in *Drosophila melanogaster* (pupal retina) has been identified. Phosphotyrosyl protein phosphatases (PTPs) are structurally diverse enzymes increasingly recognized as having a fundamental role in cellular processes including effects on metabolism, cell proliferation, and differentiation. This study presents identification of novel sequences of PTPs and their comparative homology modeling from *Drosophila melanogaster* (Dr-PTPs) and complexation with the potent inhibitor HEPES. The 3D structure was predicted based on sequence homology with bovine heart low molecular weight PTPs (Bh-PTPs). The sequence homologies are approximately 50% identical to each other and to low molecular weight protein tyrosine phosphatases (PTPs) in other species. Comparison of the 3D structures of Bh-PTPs and Dr-PTPs (primo-2) reveals a remarkable similarity having a four stranded central parallel β sheet with flanking α helices on both sides, showing two right handed β-α-β motifs. The inhibitor shows similar binding features as seen in other PTPs. The study also highlights the key catalytic residues important for target recognition and PTPs' activation. The structure guided studies of both proteins clearly reveal a common mechanism of action and inhibitor binding at the active site and will be expected to contribute toward the basic understanding of functional association of this enzyme with other molecules.

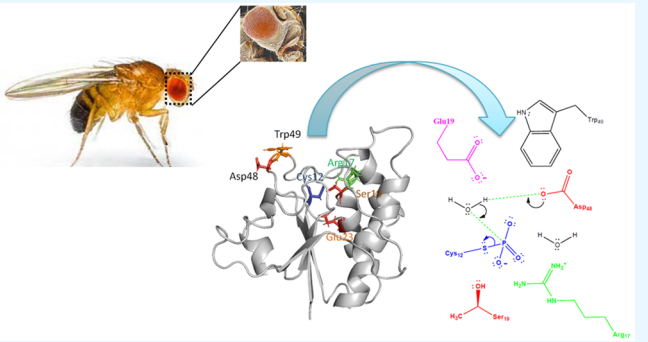

INTRODUCTION

Low molecular weight phosphotyrosine protein phosphatases (PTPs), previously known as low molecular weight acid phosphatases, catalyze the hydrolysis of tyrosine phosphorylated proteins, low molecular weight aryl phosphates, and natural and synthetic acyl phosphates.[1,2] The proteins undergoing phosphorylation during post-translation modification by acid phosphatases are little known in the literature except flavin mononucleotide (FMN). Acid phosphatases play a vital role in the biosynthesis of FMN.[3,4] Tyrosine phosphorylation plays a vital role in the regulation of the variety of developmental processes. These processes include several cell functions such as growth, cell differentiation, metabolism, cell cycle, and cytoskeletal functions. Furthermore, the phosphorylation state of tyrosine and seγ/thr of signaling proteins are controlled via specific reaction. Thus, the phosphorylation state is controlled in a very dynamic manner to avoid severe malfunction of cells.[5]

PTPs can act as tumor suppressor by inhibiting cell growth. Functionally two types of PTP sequences are conserved and well distinguished by structure comparison. The one known as classical PTPs are specific for tyrosine residues, and the other with the dual-specificity phosphates (DSPs) are essential for serine and threonine dephosphorylation. The active site (C-(X5)-R) of these PTPs contains several conserved cysteines and arginines, important for catalyzing phosphorylation processes, and thus, it plays a vital role in regulation of signal transduction. All these acid phosphatase enzymes share little sequence homology and have a different range of molecular weight (18 kDa or above), but they exhibit the same catalytic mechanism.[6,7] The structural features of low molecular weight PTPs (LMW-PTPs) comprise relatively different folds comparing from fission yeast to mammals.[8,9] The overall three-dimensional structural features contain four β sheets at the center surrounded by α helix.[6,10,11] However, several similarities can be seen in the structural features and binding

Received: July 28, 2022
Accepted: November 3, 2022
Published: December 30, 2022

https://doi.org/10.1021/acsomega.2c04760
ACS Omega 2023, 8, 1937−1945

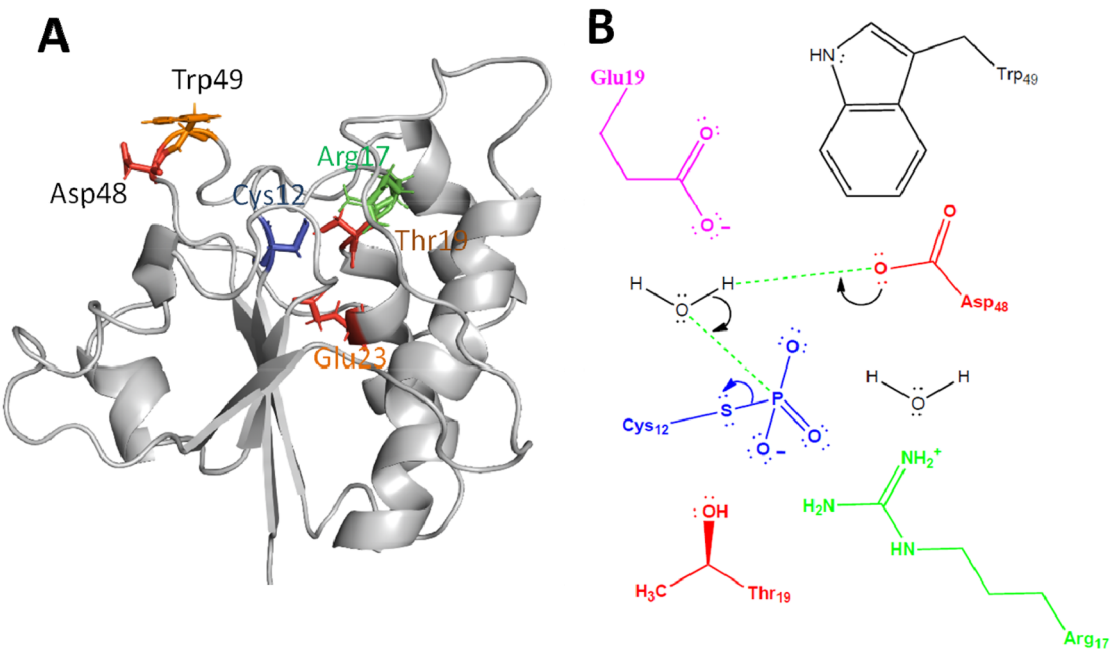

Figure 1. Catalytic mechanism of acid phosphates: (A) 3D structure (PDB: 1BVH) showing key residues important for catalytic activity and stabilization of the phosphor-cysteine intermediate. (B) Schematic diagram of different residues participating in the process of phosphorylation.

side pockets of higher molecular weight PTPs (HMW-PTPs) to LMW-PTPs.[10−15] Importantly, the conserved P-loop is stabilized by the complex hydrogen network and favors the phosphate trigonal bipyramidal transition state geometry.[16−19] Thus, all low and higher molecular weight-PTPs share an identical catalytic mechanism.[20] The enzymatic reaction is triggered by the first cysteine, where the substrate binding at the active site is stabilized by the P-loop residues via hydrogen bonding and three anionic oxygen atoms. These transient interactions orient the phosphorus atom in a feasible position for nucleophilic attack and favor the enzymatic phosphorylation reaction.[20−22] The nucleophilic attack of the thiol (Sγ) group takes place in the presence of the proton donor aspartic acid, and thus, a phosphor-cysteine intermediate is formed.[23−25] The formation of a phosphor-cysteine intermediate is also favored and stabilized by the presence of the P-loop where several residues are involved in binding and lowering the activation energy.[20] In the subsequent step, hydrolysis of the phosphor-enzyme intermediate complex via attack of water takes place, resulting in the liberation of inorganic phosphate (Pi) (Figure 1). The enzymatic phosphorylation via hydrolysis works well in the wide range of pH 5.5−7.5 from substrate.

The structural details of proteins are important parameters to understand the reactivity and stability of proteins. Several advanced techniques such as X-ray crystallography, nuclear magnetic resonance (NMR), and electron microscopy are frequently used to determine the structure of proteins. However, theoretical approaches such as comparative modeling are often used as a useful alternative to other biophysical and analytical techniques by providing insights into structural and functional aspects of proteins. In the current project, the comparative modeling technique has been used for the 3D structural prediction of sequence emerging from Primo-2 of *Drosophila melanogaster* (fruit fly) classified as the low molecular weight PTPs family (LMW-PTPs). The present work is designed to elaborate the prediction of the evolutionary context of the sequence homological ancestors, structural aspects, and active site conformational states of *Drosophila melanogaster* PTPs (Dr-PTPs) and spatial geometry formation of the active site. Dr-PTPs share 46% amino acid sequence identity with that of Bovine heart PTPs (Bh-PTPs) (PDB: 1DG9) particularly in the active site regions.

METHODOLOGY

Sequence Analysis. Sequence analysis of Dr−PTPs was obtained from the SWISS-PROT database.[26] The sequence homology from the Protein Data Bank was obtained from BLAST,[27,28] where Modeller was used for target template alignment[29] for Dr-PTPs. The program ClustalX was used for analysis of multiple sequences and adjustment of parameters made where necessary, and finally, phylogenetic lineage was established with the program PHYLIP.[30,31]

Model Building and Refinement. The three-dimensional model of Dr-PTPs was constructed using Modeller ($9V_2$) using Bh-PTPs crystal structure (PDB: 1DG9) as template model. The structure obtained was also compared with the result obtained from Alphafold2.[32,33] The program was allowed to satisfy all dihedral angle, bond, and spatial restraints and distances automatically as per default parameters. The input files consist of Dr-PTPs and Bh-PTPs aligned sequentially. Several runs of calculations were performed to get a more reliable and plausible model. The homology modeling was performed using standard parameters of calculations and known 3D structure models from the Protein Data Bank. The secondary structure elements of the model were visualized using PyMOL and MOLMOL,[16,31] and other structural statistics were performed using the PSVS site (https://montelionelab.chem.rpi.edu/PSVS/). The chemical properties and interaction of several ligands were analyzed using the program Ligand Explorer (http://ligand-expo.rcsb.org/index.html)[34] and PyMOL.[16]

Inhibitor Modeling. The identification of hotspot residues, important for target recognition and interaction was

https://doi.org/10.1021/acsomega.2c04760
ACS Omega 2023, 8, 1937−1945

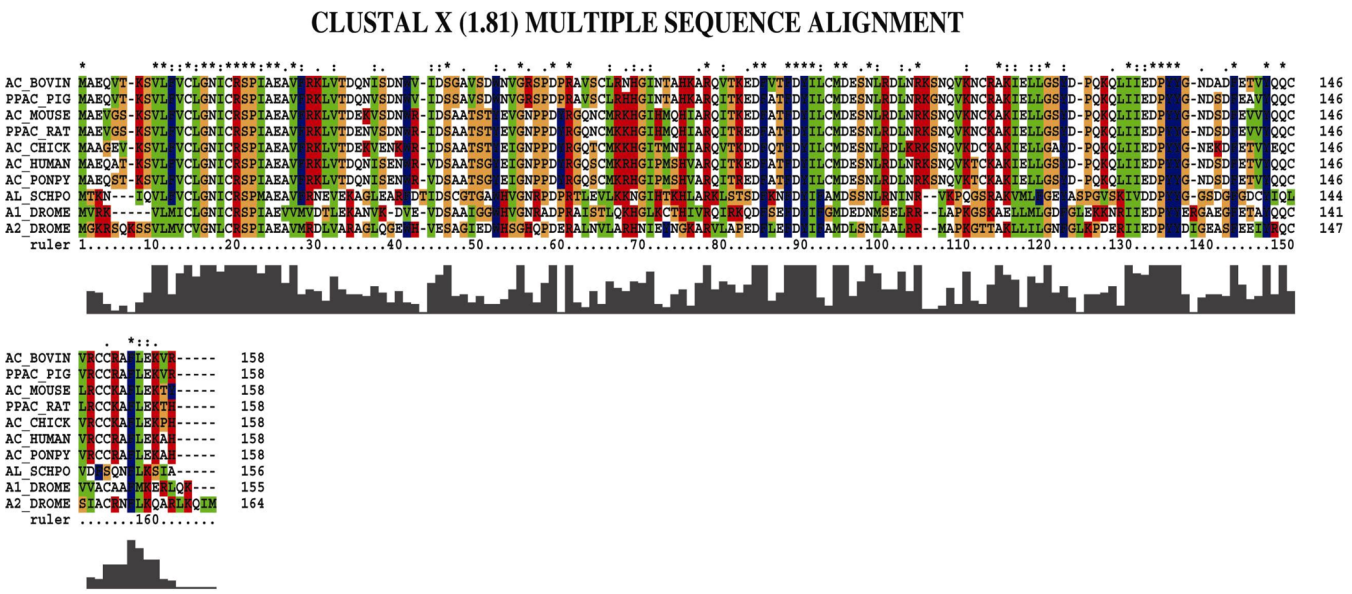

Figure 2. Multiple sequence alignment of 10 PTP sequences. Sequences are named as the SWISS-PROT entry: the first letter represents the gene; the second part represents the biological source of the gene. Symbols: "*" represents strongly conserved; "." represents weakly conserved; ":" represents identical residues.

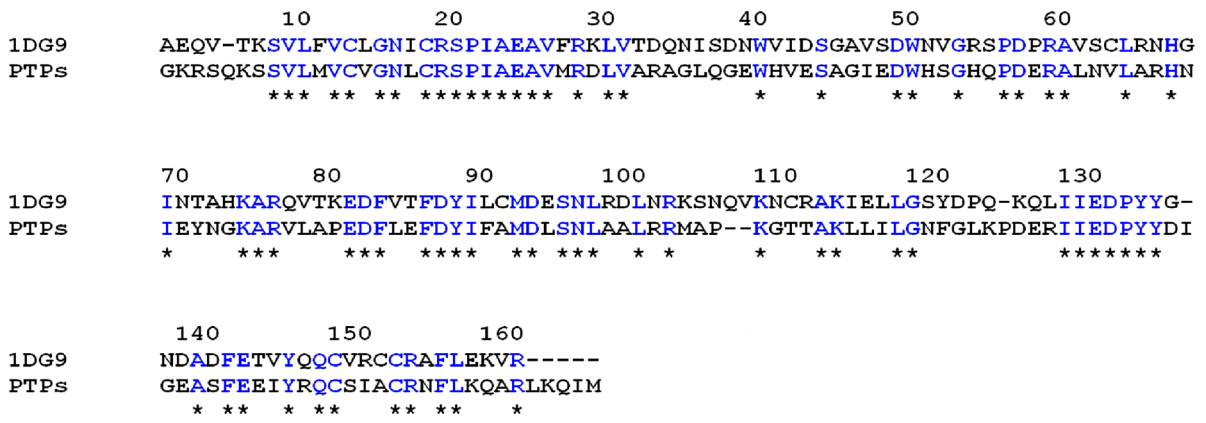

Figure 3. Pairwise sequence alignment used for building the model of Drosophila phosphatase. Target sequence represented by PTPs. Based on the structure of the bovine heart phosphatase template structure represented by 1DG9.

performed. The Dr-PTPs complexed with [N-(2-hydroxyethyl) piperazine-N-2-ethanesulfonic acid sodium salt] (HEPES) were constructed using the program Modeller where the crystal structure 1DG9 was used as template. All these ligands known as potential inhibitors were models for the active sites for Dr-PTPs. The geometrical analysis, stereochemical analysis, and all energies of bonds and dihedral restraints were analyzed. The homology models were subjected to the programs PROCHECK and ProSA for reliability of the model, secondary structure elements, backbone, and energetic architecture and fold.[35−38]

RESULTS AND DISCUSSION

Sequence Analysis. Two novel pairs of protein tyrosine phosphatases were identified in the Drosophila pupil retina. It was found that the primary sequences were approximately 50% identical and characterized as low molecular weight protein phosphatase (Figures 2 and 3). The first sequence was incorporated at primo-1 (155 amino acids) and the other encoded by primo-2 (164 amino acids).

Structure Topology. The structure of Dr-PTPs (primo-2) comprises a fold containing four central β parallel sheets gathered by α-helices: a right handed β-α-β motif. The conserved sequence known as the active site C-(X5)-R(S/T) of acid phosphatases was present as the sequence CVGNLCRS in Dr-PTPs. The active site was presented in the form of a loop extending from between β1 and helix α1 (Figure 4).

The crystal structure (PDB: IDG9) shows a complex of Bh-PTPs with HEPES, where the active site residues were interacting with the sulfonate moiety, accumulating phosphate binding manner in the pocket. All the oxygen atoms of the sulfonate group were involved in the complex hydrogen bonding network, offered by N, H, and S of the backbone residues of the active site loop and conserved arginine (Arg 18). The structural features of the sulfonate complex were found to be similar to phosphates bounded at active sites. In our case, the highest sequence similarity of Dr-PTPs' (Primo-2) primary sequence at the substrate attracting site C-(X5)-R, the tyrosine phosphorylation site RIIEDPYY was found. The 3D structure of Dr-PTPs (Primo-2) was superimposed at Bh-PTPs (PDB: 1DG9). It was found that both structures aligned

https://doi.org/10.1021/acsomega.2c04760
ACS Omega 2023, 8, 1937−1945

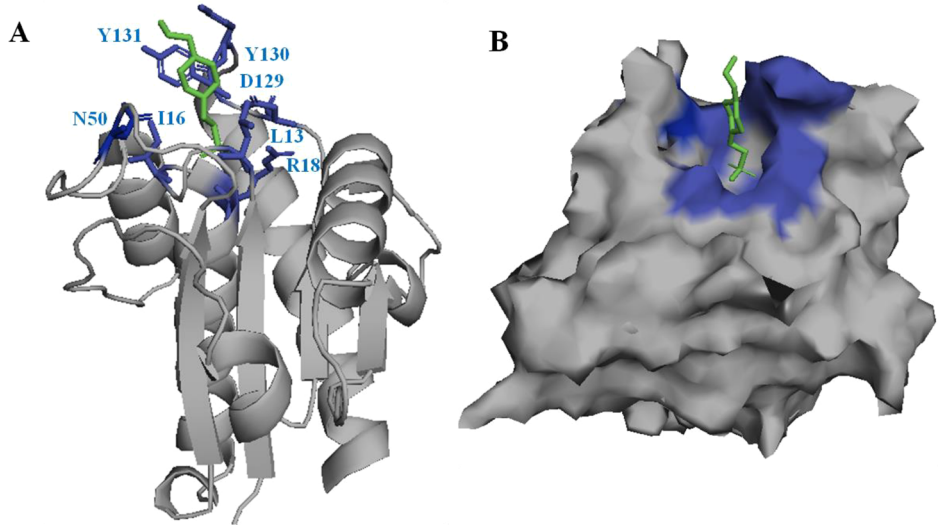

Figure 4. (A) Schematic diagram of bovine heart PTPs (1DG9) complexed with HEPES. The active site residues complexed with HEPES in 1DG9 are labeled and colored blue while the ligand HEPES is shown in green. (B) Surface representation of the active site residues making a deep groove encompassing aromatic residues (blue) while HEPES is shown green.

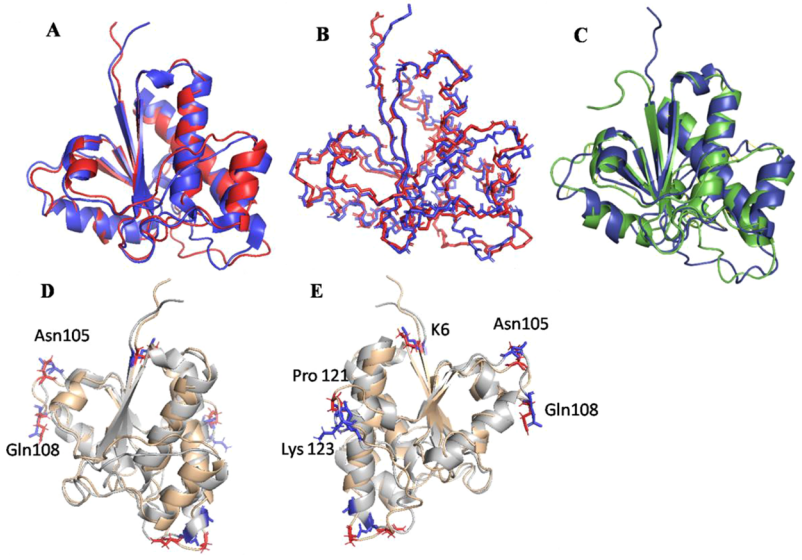

Figure 5. Structural alignment of acid phosphatases of low molecular weight phosphotyrosine phosphatase showing secondary structure elements of (A) IBVH (red) and Drosophila (blue). (B) The backbone of both proteins was aligned using the software PyMOL, and an RMSD of 1.564 Å was obtained. (C) The models obtained from Modeller and AlphaFold were compared, and an RMSD of 1.617 Å was found for Cα of secondary structure residues. (D and E) Side chains of selected residues showing different orientations after superposing the average structure from the MD simulation for 50 ns.

well for several motifs. However, regions such as Lys 6, Pro 105, Thr 108, Ile 134, Glu 136, Lys 121, Asp 123, Leu 159, and Met 163 of the Dr-PTPs' structural orientation were different from the target (Figure 5D and E). Furthermore, the sequence analysis on the basis of multiple sequence alignments and the construction of phylogenetic tree (PHYLIP package) show that both Dr-PTPs and Bh-PTPs belong to common ancestors. They are homologous sequences and members of the same subfamily as per evolutionary context (Figure 6).

TOPOLOGY OF PREDICTED HOMOLOGY MODEL OF LOW M_R DROSOPHILA PTPASE

Structure Topology. The overall secondary and tertiary structure of the Drosophila phosphatase strongly resembles the templates 1BVH, 1DG9, and 1PNT (bovine heart) and other low molecular weight phosphotyrosine protein phosphatases (Figure 5). The 3D structure was characterized with the active site end at α1 and situated close to the N terminal region followed by the P-loop and β1 strand. The active site emerges as a deep groove encompassing aromatic residues (Trp-49, Tyr-131, Tyr-132) and appears like claws while the conserved residues Asp-56 and Arg 58 of variable loops provide a network of hydrogen bonds with the other adjacent α5-helix and β4-strand. All these residues work together for target recognition and set a proper orientation of the ligand for the catalytically important residues Cys12, Cys17, and Arg18, with Asp129 (β4 extended loop) on the other end of the pocket to facilitate the protonation of the phosphorylated intermediate together with Tyr131 and Tyr132. The hydrophobicity of the active site

https://doi.org/10.1021/acsomega.2c04760
ACS Omega 2023, 8, 1937−1945

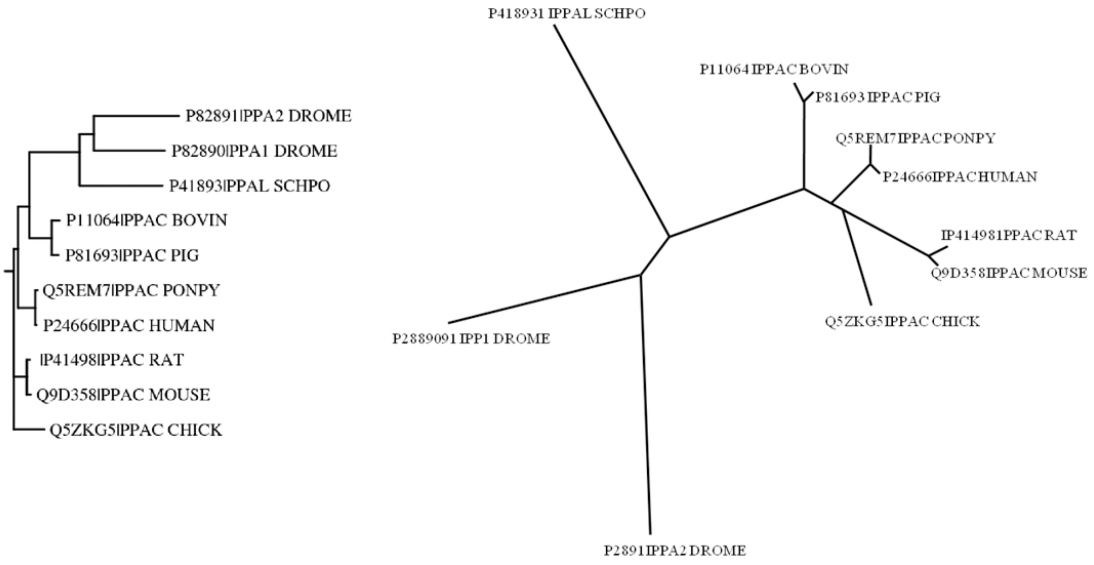

Figure 6. Dendrogram of PPA2 *Drosophila melanogaster* and homologous sequences of the same subfamily as per evolutionary context were subjected to PHYLIP, and the relationships among various forms of PPAC, PPAI, and PPA2 genes were established. The right panel represents codes of different genes of different species, while the left panel is codes representing the source of protein.

groove is maintained by several buried hydrophobic residues such as Leu 9, Val11, Phe82, Ile 88, Leu 99, and Lys 102.

Quality of Model. The different aspects of the structure of Dr-PTPs were validated using different tools. The model obtained from Modeller was compared with the AlphaFold program (Figures 5C and S2). The stereochemical outcomes were analyzed using the software PROCHECK, where the restraints obtained were compared to the stereochemical properties of Bh-PTPs. The degree of violation of secondary structure elements was evaluated using a Ramachandran plot where 94% of the regions were found in allowed regions and no dihedral regions in disallowed regions, confirming the validity of the model.

The 10 best structures of the Dr-PTPs were compared with the Bh-PTPs' crystal structure, both free and complexed with HEPES. The RMSDs based on the backbone (α-carbon) were found to be 0.26 and 0.49 Å in the presence and absence of complexation (Table 1), respectively. These observations

Table 1

Template	Target	RMSD
Bovine heart PTPs (1BVH) without inhibitor	Drosophila PTPs	0.4840
Bovine heart PTPs (1DG9) with inhibitor (HEPES)	Drosophila PTPs	0.2549
Bovine heart PTPs (1PNT) with inhibitor (PO_4)	Drosophila PTPs	0.1536

further confirmed the validity of the model besides the higher sequence identity. However, the conformational variability can be seen in several regions (1−6, 105−108, 134−136, and 121−123) due to presence of different amino acids inducing different orientations (Figure 7A).

The energy of the fold was calculated using the program ProSA where Bh-PTPs' crystal structure was used as template. The comparison of energy was explored as shown by the energy graph (Figure 8).

Active Site and Protein Inhibitor Interactions. The structural similarity of Dr-Ptps and Bh-Ptps and the conformational resemblance of the active site demonstrate the identity

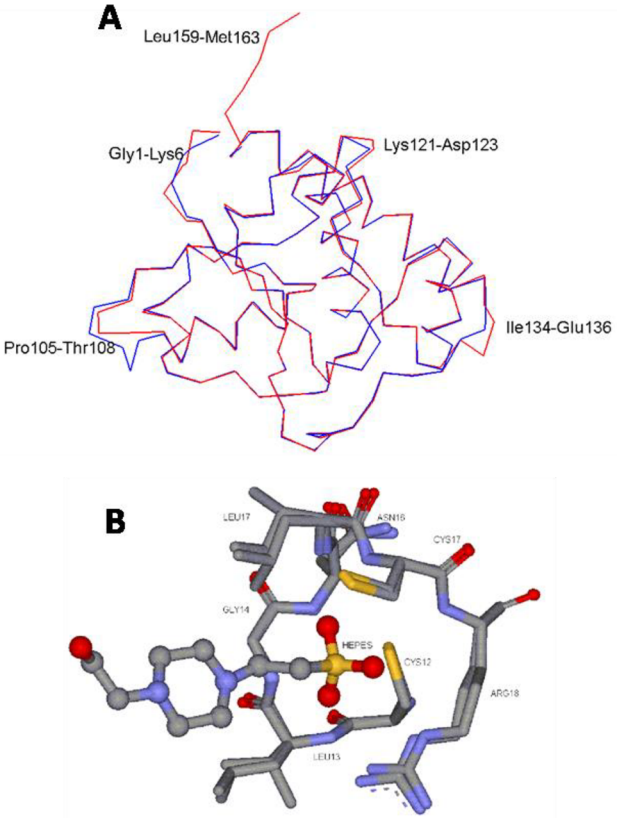

Figure 7. Aligned structures of the template (Bh-PTPs) and Dr-PTPs (A). The active site is 100% superimposed in both structures, as shown in (B). The active site is represented in sticks, whereas the inhibitor (HEPES) is represented in ball and sticks style.

of the catalytic mechanism. The catalytic reaction is triggered by the nucleophilic attack by Cys 3. The phosphate group at the tyrosine group of the ligand or substrate is bound at the active site in an orientation such that all three oxygen atoms form hydrogen bonding with P-loop residues, making feasible the nucleophilic attack at the phospho group by Cys3, Cys14,

https://doi.org/10.1021/acsomega.2c04760
ACS Omega 2023, 8, 1937−1945

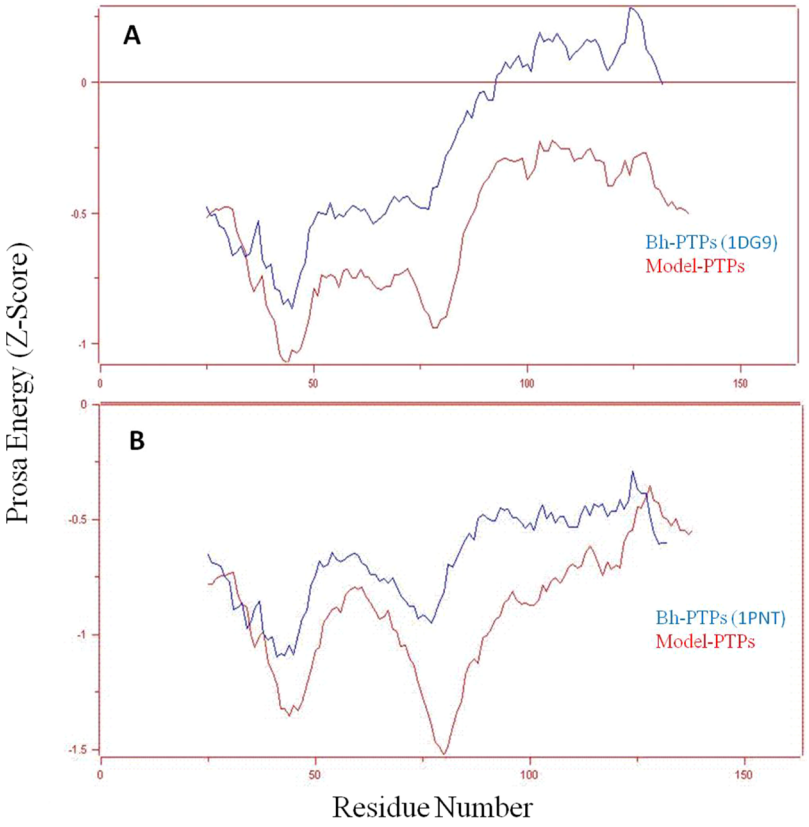

Figure 8. Comparison of the energy of folding using the ProSA program: The figure shows a comparison of combined surface and pairing energy plots (ProSA Energy Z-Score) examined as a function of residue. (A) Comparison of Bh-PTPs (PDB: 1DG9, blue) and model PTPs (red). (B) Bh-PTPs (PDB: 1PNT, blue) and model PTPs (red).

Table 2. Ligand Oxygen (HEPES)-Protein Nitrogen Bond Length in PTPs Complexes

Bovine Heart PTPs Complex with HEPES			Drosophila PTPs Complex with HEPES		
1DG9	Amino acids	Distance (Å)	Model PTPs	Amino acids	Distance (Å)
EPE201:O1S	LEU13:N	3.17	EPE164:O1S	VA14:N	3.18
EPE201:O1S	GLY14:N	2.98	EPE164:O1S	GLY15:N	3.02
EPE201:O2S	ILE16:N	3.04	EPE164:C2	LEU17:N	3.06
EPE201:O2S	CYS17:N	2.88	EPE164:O2S	CYS18:N	2.88
EPE201:O1S	ARG 18:NH2	2.93	EPE164:O2S	ARG19:N	3.26
EPE201:O3S	ARG18:N	3.2	EPE164:O1S	ARG19:NH2	3.1
EPE201:O3S	ARG18:NE	2.94	EPE164:O3S	ARG19:NE	2.9
			EPE164:N1	EPE164:N4	2.99
			EPE164:N4	EPE164:N1	2.99

Table 3. Ligand Oxygen (PO_4)-Protein Nitrogen Bond Length in PTPs Complexes

Bovine Heart PTPs Complex with PO_4			Drosophila PTPs Complex with PO_4		
1PNT	Amino acids	Distance (Å)	PPD10	Amino acids	Distance (Å)
PO4158:O3	LEU13:N	3.24	PO4164:O3	VAL14:N	3.24
PO4158:O3	GLY14:N	2.87	PO4164:O3	GLY15:N	2.91
PO4158:O2	ILE16:N	2.87	PO4164:O2	ASN16:N	3.28
PO4158:O2	CYS17:N	2.73	PO4164:O2	LEU17:N	2.9
PO4158:O3	ARG18:NH2	2.92	PO4164:O2	CYS18:N	2.74
PO4158:O4	ARG18:N	3.29	PO4164:O3	ARG19:NH2	3.06
PO4158:O4	ARG18:NE	2.78	PO4164:O4	ARG19:NE	2.94
			PO4164:O1	TYR131:OH	3.17
			PO4164:O3	PO4164:O4	2.51
			PO4164:O4	PO4164:O3	2.51

https://doi.org/10.1021/acsomega.2c04760
ACS Omega 2023, 8, 1937−1945

Cys16, and Cys18 where Asp 129 works as proton donor resulting in the formation of the phosphoenzyme intermediate.[17,19] Hydrolytic cleavage of the intermediate takes place, resulting in the formation of inorganic phosphate.

The complexation of HEPES at the active site of the enzyme is stabilized by hydrophilic interactions such as hydrogen bonding and hydrophobic electrostatic interactions, and thus, it acts as a potent inhibitor. In Bh-PTPs (PDB: IDG9), the inhibitor HEPES is stabilized by forming seven hydrogen bonds with active site residues of the enzyme. In a similar fashion, nine hydrogen bonds were observed in Dr-PTPase. In the case of Bh-PTPs, residues such as Leu 13, Gly 14, Ile 16, Cys 17, and Arg 18 are involved in hydrogen bonding with the inhibitor HEPES. Only three oxygens of HEPES are involved in hydrogen bonding with the active site residues of PTPs (Tables 2 and 3). Residues such as Val 14, Gly 15, Leu 17, Cys 18, and Arg 19 participate in the hydrogen bonding of Dr-PTPs (target). Two nitrogen atoms and three oxygen atoms of HEPES (inhibitor) are involved in hydrogen bonding with the active site residues of PTPase (Figure 7B).

The stabilization of HEPES for complexation with Bh-PTPs is favored by hydrophobic interaction by residues Ile 16 and Tyr 131, while, in Dr-PTPs, Leu 17, His 51, and Tyr 131 are involved in hydrophobic interactions.

CONCLUSION

The sequence and secondary and tertiary structural similarities were studied in the proteins Dr-PTPs and Bh-PTPs. The sequences of both proteins were found homologous for the overall motifs and more especially for the active site motif represented by the conserved residues C-(X5)-R. The comparative analysis of sequences is evident in the fact that this strong signature (CXXXXXR) at the active site is the characteristic of low molecular weight phosphotyrosine protein phosphatases. It was found that residues in the 10−27, 81−88, and 127−130 regions were highly conserved with low molecular weight PTPs. The structures obtained for this novel sequence were found to be reliable and valid based on analyses performed by various protein structure validation tools, as shown by the Ramachandran plot, PROCHECK, the energy of the fold, and comparative analysis with other template crystal structures. The complexation profile of Dr-PTPs was also established based on the potent inhibitor HEPES. The overall stabilization factors important for the inhibitor complexation were studied and compared with the known literature. We found that the strong conformational similarity of Dr-PTPs with other homologous PTPs may share the same types of inhibitors exclusively considered to inhibit low molecular weight phosphotyrosine protein PTPs. All these structural details obtained from the model are important for scheming further specific inhibitors. They can be used as an additional probe to decipher the discrete biological role of the low molecular weight phosphotyrosine PTPs family and to explore the potential use of these macromolecular species as therapeutic targets.

ASSOCIATED CONTENT

Data Availability Statement

The data acquired in this manuscript is available for method validation and reproducibility of the results. We used softwares Clustalx,[30,39] Modeler,[29] and Procheck[35] for making sequence alignments and modeling studies. The data obtained is available in the Supporting Information or otherwise mentioned in the article.

Supporting Information

The Supporting Information is available free of charge at https://pubs.acs.org/doi/10.1021/acsomega.2c04760.

The MS simulation results of Drosophila phosphatase and bovine heart phosphatase (Figure S1). The result of the model obtained from alphafold2 (Figure S2). (PDF)

AUTHOR INFORMATION

Corresponding Authors

Narcisa Vrinceanu − *Faculty of Engineering, Department of Industrial Machines and Equipment, "Lucian Blaga" University of Sibiu, Sibiu 550024, Romania*; Email: vrinceanu.narcisai@ulbsibiu.ro

Anwar Iqbal − *Department of Chemical Sciences, University of Lakki Marwat, Lakki Marwat 28420, Pakistan*; orcid.org/0000-0002-3595-0511; Phone: +92 3325369489; Email: anwar@ulm.edu.pk

Authors

Rubina Naz − *Institute of Chemical Sciences, Gomal University, Dera Ismail Khan 29050, Pakistan*

Asma Saeed − *Department of Biological Sciences, Gomal University, Dera Ismail Khan 29050, Pakistan*

Vineet Tirth − *Mechanical Engineering Department, College of Engineering, King Khalid University, Abha 61421, Kingdom of Saudi Arabia; Research Center for Advanced Materials Science (RCAMS), King Khalid University, Abha 61413 Asir, Kingdom of Saudi Arabia*

Neeraj Kumar Shukla − *Mechanical Engineering Department, College of Engineering, King Khalid University, Abha 61421, Kingdom of Saudi Arabia*

Abdulilah Mohammad Mayet − *Mechanical Engineering Department, College of Engineering, King Khalid University, Abha 61421, Kingdom of Saudi Arabia;* orcid.org/0000-0001-7739-0105

Alamzeb Khan − *Department of Pediatrics, Yale School of Medicine, Yale University, New Haven, Connecticut 06511, United States*

Mihaela Racheriu − *Medicine Faculty, "Lucian Blaga" University of Sibiu, Sibiu 550245, Romania*

Tahira Amir − *Department of Chemistry, University of Wah, Wah 47040, Pakistan*

Complete contact information is available at: https://pubs.acs.org/10.1021/acsomega.2c04760

Notes

The authors declare no competing financial interest.

ACKNOWLEDGMENTS

The authors extend their appreciation to the Deanship of Scientific Research at King Khalid University Abha for funding this work through a General Research Project under grant number GRP/256/43. Project financed by Lucian Blaga University of Sibiu through research grant LBUS-IRG-2022-08.

REFERENCES

(1) Kumar, A.; Rana, D.; Rana, R.; Bhatia, R. Protein Tyrosine Phosphatase (PTP1B): A Promising Drug Target Against Life-Threatening Ailments. *Curr. Mol. Pharmacol.* **2020**, *13* (1), 17−30.

(2) Tonks, N. K. Protein Tyrosine Phosphatases: From Genes, to Function, to Disease. *Nature Reviews Molecular Cell Biology* **2006**, *7*, 833−846, DOI: 10.1038/nrm2039.
(3) Sa, N.; Rawat, R.; Thornburg, C.; Walker, K. D.; Roje, S. Identification and Characterization of the Missing Phosphatase on the Riboflavin Biosynthesis Pathway in *Arabidopsis Thaliana*. *Plant J.* **2016**, *88* (5), 705−716.
(4) Niu, R. J.; Zheng, Q. C.; Zhang, H. X. Molecular Basis of the Recognition of FMN by a HAD Phosphatase TON_0338. *J. Mol. Graph. Model.* **2016**, *69*, 17−25.
(5) Bull, H.; Murray, P. G.; Thomas, D.; Fraser, A. M.; Nelson, P. N. Acid Phosphatases. *Journal of Clinical Pathology - Molecular Pathology* **2002**, 65−72, DOI: 10.1136/mp.55.2.65.
(6) Logan, T. M.; Zhou, M. M.; Nettesheim, D. G.; Meadows, R. P.; Fesik, S. W.; Van Etten, R. L. Solution Structure of a Low Molecular Weight Protein Tyrosine Phosphatase. *Biochemistry* **1994**, *33* (37), 11087−11096.
(7) Zhang, M.; Van Etten, R. L.; Stauffacher, C. V. Crystal Structure of Bovine Heart Phosphotyrosyl Phosphatase at 2.2-Å Resolution. *Biochemistry* **1994**, *33* (37), 11097−11105.
(8) Zhang, Z. Y. Protein-Tyrosine Phosphatases: Biological Function, Structural Characteristics, and Mechanism of Catalysis. *Critical Reviews in Biochemistry and Molecular Biology. Crit Rev. Biochem Mol. Biol.* **1998**, *33*, 1−52.
(9) Granjeiro, J. M.; Miranda, M. A.; Maia, M. D. G. S. T.; Ferreira, C. V.; Taga, E. M.; Aoyama, H.; Volpe, P. L. O. Effect of Homologous Series of N-Alkyl Sulfates and N-Alkyl Trimethylammonium Bromides on Low Molecular Mass Protein Tyrosine Phosphatase Activity. *Mol. Cell. Biochem.* **2004**, *265* (1−2), 133−140.
(10) Evans, B.; Tishmack, P. A.; Pokalsky, C.; Zhang, M.; Van Etten, R. L. Site-Directed Mutagenesis, Kinetic, and Spectroscopic Studies of the P- Loop Residues in a Low Molecular Weight Protein Tyrosine Phosphatase. *Biochemistry* **1996**, *35* (42), 13609−13617.
(11) Tailor, P.; Gilman, J.; Williams, S.; Couture, C.; Mustelin, T. Regulation of the Low Molecular Weight Phosphotyrosine Phosphatase by Phosphorylation at Tyrosines 131 and 132. *J. Biol. Chem.* **1997**, *272* (9), 5371−5374.
(12) Yuvaniyama, J.; Denu, J. M.; Dixon, J. E.; Saper, M. A. Crystal Structure of the Dual Specificity Protein Phosphatase VHR. *Science (80-.)* **1996**, *272* (5266), 1328−1331.
(13) Nam, H.-J.; Poy, F.; Krueger, N. X.; Saito, H.; Frederick, C. A. Crystal Structure of the Tandem Phosphatase Domains of RPTP LAR. *Cell* **1999**, *97* (4), 449−457.
(14) Kennelly, P. J. Life among the Primitives: Protein O-Phosphatases in Prokaryotes. *Front. Biosci.* **1999**, *4* (1−3), d372.
(15) Hoffmann, K. M. V.; Tonks, N. K.; Barford, D. The Crystal Structure of Domain 1 of Receptor Protein-Tyrosine Phosphatase μ. *J. Biol. Chem.* **1997**, *272* (44), 27505−27508.
(16) Glover, N. R.; Tracey, A. S. The Phosphatase Domains of LAR, CD45, and PTP1B: Structural Correlations with Peptide-Based Inhibitors 1. *Biochem. Cell Biol.* **2000**, *78* (1), 39−50.
(17) Zhang, M.; Stauffacher, C. V.; Lin, D.; Van Etten, R. L. Crystal Structure of a Human Low Molecular Weight Phosphotyrosyl Phosphatase. *J. Biol. Chem.* **1998**, *273* (34), 21714−21720.
(18) Wang, S.; Tabernero, L.; Zhang, M.; Harms, E.; Van Etten, R. L.; Stauffacher, C. V. Crystal Structures of a Low-Molecular Weight Protein Tyrosine Phosphatase from Saccharomyces Cerevisiae and Its Complex with the Substrate P-Nitrophenyl Phosphate. *Biochemistry* **2000**, *39* (8), 1903−1914.
(19) Zhang, M.; Zhou, M.; Van Etten, R. L.; Stauffacher, C. V. Crystal Structure of Bovine Low Molecular Weight Phosphotyrosyl Phosphatase Complexed with the Transition State Analog Vanadate. *Biochemistry* **1997**, *36* (1), 15−23.
(20) Jia, Z.; Barford, D.; Flint, A. J.; Tonks, N. K. Structural Basis for Phosphotyrosine Peptide Recognition by Protein Tyrosine Phosphatase 1B. *Science (80-.)* **1995**, *268* (5218), 1754−1758.
(21) Wo, Y. Y. P.; McCormack, A. L.; Shabanowitz, J.; Hunt, D. F.; Davis, J. P.; Mitchell, G. L.; Van Etten, R. L. Sequencing, Cloning, and Expression of Human Red Cell-Type Acid Phosphatase, a Cytoplasmic Phosphotyrosyl Protein Phosphatase. *J. Biol. Chem.* **1992**, *267* (15), 10856−10865.
(22) Zhang, Z.; Harms, E.; Van Etten, R. L. Asp129 of Low Molecular Weight Protein Tyrosine Phosphatase Is Involved in Leaving Group Protonation. *J. Biol. Chem.* **1994**, *269* (42), 25947−25950.
(23) Lau, K. H. W.; Farley, J. R.; Baylink, D. J. Phosphotyrosyl Protein Phosphatases. *Biochem. J.* **1989**, *257*, 23−36.
(24) Wu, L.; Zhang, Z. Y. Probing the Function of Asp128 in the Low Molecular Weight Protein-Tyrosine Phosphatase-Catalyzed Reaction. A Pre-Steady-State and Steady-State Kinetic Investigation. *Biochemistry* **1996**, *35* (17), 5426−5434.
(25) Zhang, Z. Y.; Van Etten, R. L. Leaving Group Dependence and Proton Inventory Studies of the Phosphorylation of a Cytoplasmic Phosphotyrosyl Protein Phosphatase from Bovine Heart. *Biochemistry* **1991**, *30* (37), 8954−8959.
(26) Bairoch, A.; Apweiler, R. The SWISS-PROT Protein Sequence Database and Its Supplement TrEMBL in 2000. *Nucleic Acids Res.* **2000**, *28*, 45−48, DOI: 10.1093/nar/28.1.45.
(27) Boratyn, G. M.; Camacho, C.; Cooper, P. S.; Coulouris, G.; Fong, A.; Ma, N.; Madden, T. L.; Matten, W. T.; McGinnis, S. D.; Merezhuk, Y.; Raytselis, Y.; Sayers, E. W.; Tao, T.; Ye, J.; Zaretskaya, I. BLAST: A More Efficient Report with Usability Improvements. *Nucleic Acids Res.* **2013**, *41* (W1), W29−W33, DOI: 10.1093/nar/gkt282.
(28) Morgulis, A.; Coulouris, G.; Raytselis, Y.; Madden, T. L.; Agarwala, R.; Schäffer, A. A. Database Indexing for Production MegaBLAST Searches. *Bioinformatics; Bioinformatics* **2008**, *24*, 1757−1764.
(29) Eswar, N.; Webb, B.; Marti-Renom, M. A.; Madhusudhan, M. S.; Eramian, D.; Shen, M.; Pieper, U.; Sali, A. Comparative Protein Structure Modeling Using Modeller. *Curr. Protoc. Bioinformatics* **2006**, *15* (1), 5.6.1−5.6.30, DOI: 10.1002/0471250953.bi0506s15.
(30) Wang, Y.; Wu, H.; Cai, Y. A Benchmark Study of Sequence Alignment Methods for Protein Clustering. *BMC Bioinformatics* **2018**, *19* (S19), 529.
(31) Shimada, M. K.; Nishida, T. A Modification of the PHYLIP Program: A Solution for the Redundant Cluster Problem, and an Implementation of an Automatic Bootstrapping on Trees Inferred from Original Data. *Mol. Phylogenet. Evol.* **2017**, *109*, 409−414.
(32) Webb, B.; Sali, A. Comparative Protein Structure Modeling Using MODELLER. *Curr. Protoc. Bioinforma.* **2016**, *54*, 5.6.1−5.6.37.
(33) Jumper, J.; Evans, R.; Pritzel, A.; Green, T.; Figurnov, M.; Ronneberger, O.; Tunyasuvunakool, K.; Bates, R.; Žídek, A.; Potapenko, A.; Bridgland, A.; Meyer, C.; Kohl, S. A. A.; Ballard, A. J.; Cowie, A.; Romera-Paredes, B.; Nikolov, S.; Jain, R.; Adler, J.; Back, T.; Petersen, S.; Reiman, D.; Clancy, E.; Zielinski, M.; Steinegger, M.; Pacholska, M.; Berghammer, T.; Bodenstein, S.; Silver, D.; Vinyals, O.; Senior, A. W.; Kavukcuoglu, K.; Kohli, P.; Hassabis, D. Highly Accurate Protein Structure Prediction with AlphaFold. *Nature* **2021**, *596* (7873), 583−589.
(34) Moreland, J. L.; Gramada, A.; Buzko, O. V.; Zhang, Q.; Bourne, P. E. The Molecular Biology Toolkit (MBT): A Modular Platform Fro Developing Molecular Visualization Applications. *BMC Bioinformatics* **2005**, *6* (1), 21.
(35) Laskowski, R. A.; MacArthur, M. W.; Moss, D. S.; Thornton, J. M. PROCHECK: A Program to Check the Stereochemical Quality of Protein Structures. *J. Appl. Crystallogr.* **1993**, *26* (2), 283−291.
(36) Laskowski, R. A.; Rullmann, J. A. C.; MacArthur, M. W.; Kaptein, R.; Thornton, J. M. AQUA and PROCHECK-NMR: Programs for Checking the Quality of Protein Structures Solved by NMR. *J. Biomol. NMR* **1996**, *8* (4), 477−486.
(37) Furey, W.; Cowtan, K. D.; Zhang, K. Y. J.; Main, P.; Brunger, A. T.; Adams, P. D.; DeLano, W. L.; Gros, P.; Grosse-Kunstleve, R. W.; Jiang, J.-S.; Pannu, N. S.; Read, R. J.; Rice, L. M.; Simonson, T.; Tronrud, D. E.; Ten Eyck, L. F.; Lamzin, V. S.; Perrakis, A.; Wilson, K. S.; Laskowski, R. A.; MacArthur, M. W.; Thornton, J. M.; Kraulis, P. J.; Richardson, D. C.; Richardson, J. S.; Kabsch, W.; Sheldrick, G. M. Programs and Program Systems in Wide Use. In *International*

https://doi.org/10.1021/acsomega.2c04760
ACS Omega 2023, 8, 1937−1945

Tables for Crystallography; International Union of Crystallography, 2006; pp 695−743. DOI: 10.1107/9780955360206000724.
(38) Wiederstein, M.; Sippl, M. J. ProSA-Web: Interactive Web Service for the Recognition of Errors in Three-Dimensional Structures of Proteins. *Nucleic Acids Res.* **2007**, *35* (SUPPL.2), W407.
(39) Chenna, R.; Sugawara, H.; Koike, T.; Lopez, R.; Gibson, T. J.; Higgins, D. G.; Thompson, J. D. Multiple Sequence Alignment with the Clustal Series of Programs. *Nucleic Acids Res.* **2003**, *31* (13), 3497−3500.

https://doi.org/10.1021/acsomega.2c04760
ACS Omega 2023, 8, 1937−1945